

Crystallization kinetics and nucleation parameters of Nylon 6 and poly(ethylene-co-glycidyl methacrylate) blend

Jiann-Wen Huang^{a,*}, Ching-Chih Chang^b, Chiun-Chia Kang^c, Mou-Yung Yeh^{d,e}

^a Department of Styling & Cosmetology, Tainan University of Technology,
529 Chung Cheng Road, Yung Kang City 710, Taiwan, ROC

^b Department of International Business Management, Tainan University of Technology,
529 Chung Cheng Road, Yung Kang City 710, Taiwan, ROC

^c R&D Center, Hi-End Polymer Film Co., Ltd., 15-1 Sin Jhong Road, Sin Ying City 730, Taiwan

^d Department of Chemistry, National Cheng Kung University, No. 1, University Road,
Tainan City 701, Taiwan, ROC

^e Sustainable Environment Research Centre, National Cheng Kung University, Taiwan

Received 8 October 2007; received in revised form 2 December 2007; accepted 3 December 2007

Available online 8 December 2007

Abstract

Blend of Nylon 6 and poly(ethylene-co-glycidyl methacrylate) (PEGMA) were prepared by a twin-screw extruder. Morphology observed with scanning electron microscopies (SEM) show PEGMA is well dispersed in Nylon 6 matrix. Isothermal and nonisothermal crystallization of the blend was investigated by differential scanning calorimeter (DSC) and crystallization kinetics was described by Avrami and Tobin models. Equilibrium melting temperatures were estimated from linear Hoffman–Weeks relationship. All analyses showed that the reaction between PEGMA and Nylon 6 reduced the molecular mobility and reduced the crystallization rate. Expand K_g and U^* in the Hoffman–Lauritzen equation by Vyazovkin's method demonstrated that Nylon 6/PEGMA had higher K_g and U^* values and provided another supportive evidence to the above interpretation. © 2007 Elsevier B.V. All rights reserved.

Keywords: Nylon 6; Isothermal crystallization; Nonisothermal crystallization Hoffman–Lauritzen; Vyazovkin

1. Introduction

Miscibility between components in a polymer blend is a critical factor, which influences properties of the blend [1,2]. Reactive compatibilization is an approach that allows one to compatibilize immiscible blends by generating interfacial agents in situ via a chemical reaction between the constituent components during mixing process. These in situ formed agents tend to stay at the interface, as the reaction between functional groups occurs at the interface, and thus can act as effective compatibilizers between two immiscible polymers.

Nylon 6 is one of the important classes of engineering plastics with excellent solvent resistance and good processibility. However, most polyamides have a number of drawbacks, including

low heat deflection temperature, poor dimensional stability, and low impact strength.

Poly(ethylene-co-glycidyl methacrylate) (PEGMA) is a copolymer of ethylene and glycidyl methacrylate with epoxy groups. The epoxy groups can react with functional groups of carboxyl, hydroxyl, or amines and PEGMA has been processed as compatibilizer for polar–nonpolar blends such as PBT/polypropylene [7], PET/polyethylene [8–11] and Nylon 6/PP [12]. Rubbery PEGMA has also been extensively used as an impact modifier for engineering plastic because of its good miscibility with the matrix such as poly(butylene terephthalate) (PBT) [3], poly(ethylene terephthalate) (PET) [4], poly(phenylene sulfide) (PPS) [5] and polyamides [6].

The presence of a second component in a blend affects not only the mechanical properties but also crystallization kinetics of the blend. In this article, isothermal and nonisothermal crystallization kinetics of Nylon 6 and PEGMA blend were studied by Avrami [15–17] and Tobin [18–20] mod-

* Corresponding author. Fax: +886 6 2433812.

E-mail address: jw.huang@msa.hinet.net (J.-W. Huang).

els. The equilibrium melting temperature (T_m^0) was calculated by linear Hoffman–Weeks equation [14]. The parameters of Hoffman–Lauritzen equation [13] were estimated by Kishore and Vasanthakumari [21], Lim et al. [22], and Vyazovkin's et al. [23,24] methods.

2. Experimental

2.1. Materials

Commercial grade Nylon 6 was supplied by BASF (Ulramid® B35) which had a number-average molecular weight of 24,000 and relative viscosity of 3.3 (1 g/dl in sulfuric acid). PEGMA was purchased from Sumitomo Chemical Co Ltd. (CG5004) which contained 81 wt% ethylene and 19 wt% glycidyl methacrylate, and had a melting flow index (MFI) of 180 g (2.16 kgf/190 °C, ASTM D1238). All materials were used as received without purification.

2.2. Sample preparation

All materials were dried at 323 K in a vacuum oven for 48 h before compounding. Nylon 6 and 20 wt% PEGMA were compounded with a twin-screw extruder (Continent Machinery Company, Model CM-MTE, $L/D = 32$, $D = 40$ mm) at 523 K with 300 rpm to make blends of Nylon 6/PEGMA. Twenty percent of PEGMA was chosen to make wide enough difference from neat Nylon 6 to have measurable effects. But, at the same time, not to change the processing condition too much so that a meaningful comparison can be made. For comparison, the neat Nylon 6 was also compounded by the extruder and went through similar thermal condition.

2.3. Morphology

Samples were fractured in liquid nitrogen to examine the morphology roughly normal to the extrusion direction with scanning electron microscope (HITACHI, S-3500).

2.4. Characterizations

The differential scanning calorimeter (DSC), PerkinElmer Pyris 1 DSC was calibrated by using indium standard and with a sample weight of 8–10 mg. All operations were executed in a nitrogen atmosphere. Before collecting the data of isothermal crystallization, the samples were heated to 523 K and held in the molten state for 5 min to eliminate the influence of thermal history. The sample melts were then subsequently quenched at a rate of 100 K/min to reach the specific temperatures. After the completion of isothermal crystallization, the samples were heated to 523 K at a rate of 10 °C/min to measure the melting temperatures. Nonisothermal crystallization was carried out by heating the samples to 523 K and held in the molten state for 5 min to eliminate the influence of thermal history. The sample melts were then subsequently cooled to 323 K at a heating rate of 10, 20, 30 and 40 K/min.

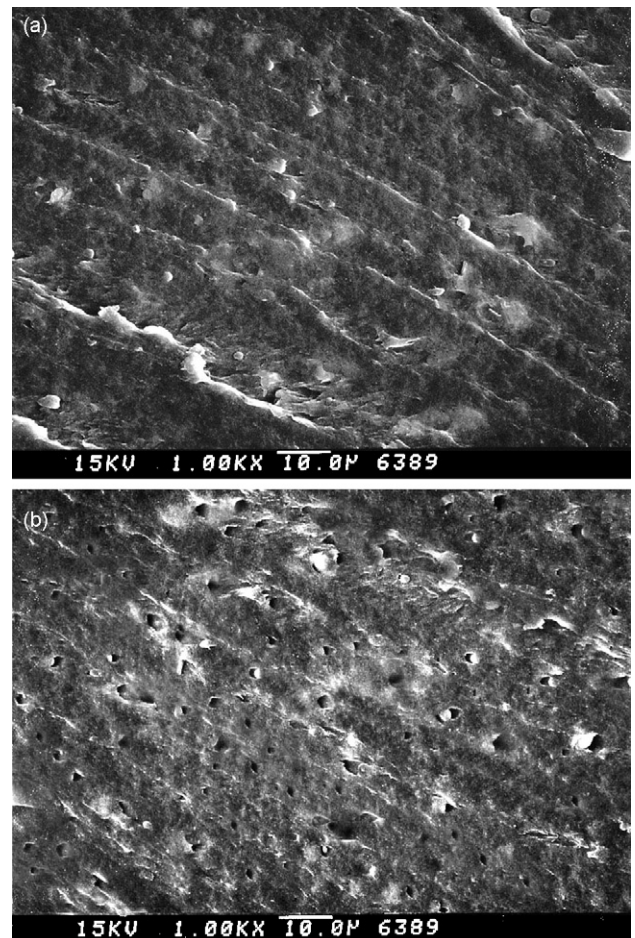


Fig. 1. SEM micrograph of Nylon 6/PEGMA blend. (a) Original specimen, (b) etched by toluene.

3. Results and discussion

3.1. Morphology

The fractured surface of the Nylon 6/PEGMA blend is shown in Fig. 1. The fine particles of PEGMA are well dispersed in

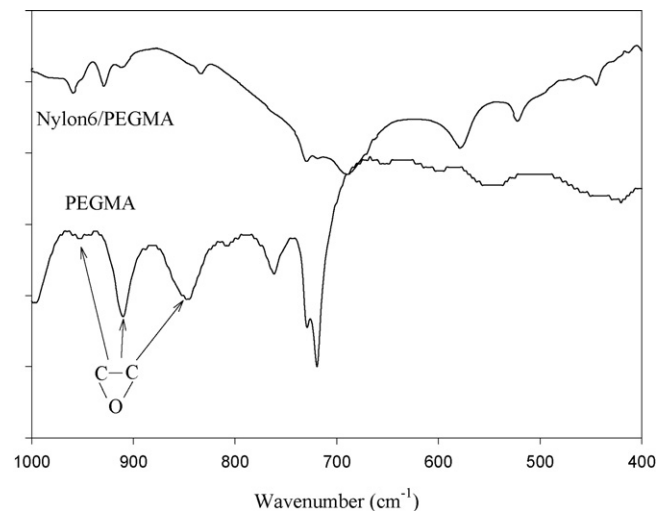


Fig. 2. IR spectrum of PEGMA and Nylon 6/PEGMA.

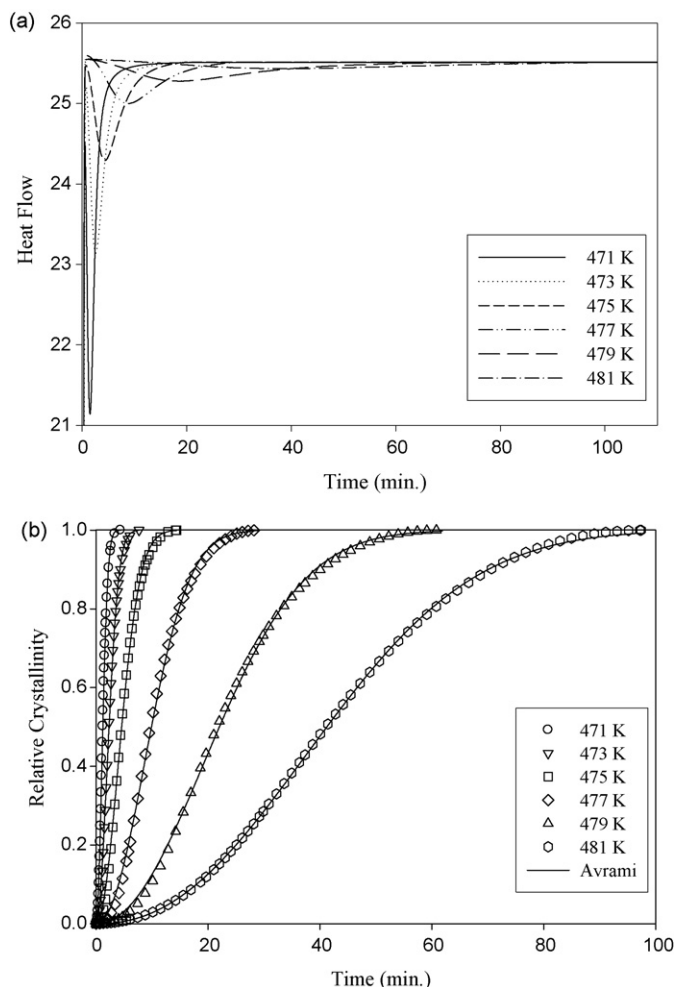


Fig. 4. DSC isothermal measurement. (a) Heat flow, and (b) relative crystallinity as a function of crystallization time and fitted by Avrami models.

that $1/t_{1/2}^i$ of Nylon 6 decreased when PEGMA was added. Such a decrease in crystallization rate may be accounted for by the increase of the blend viscosity due to reactions between Nylon 6 and PEGMA and the concurrent reduction of the molecular mobility.

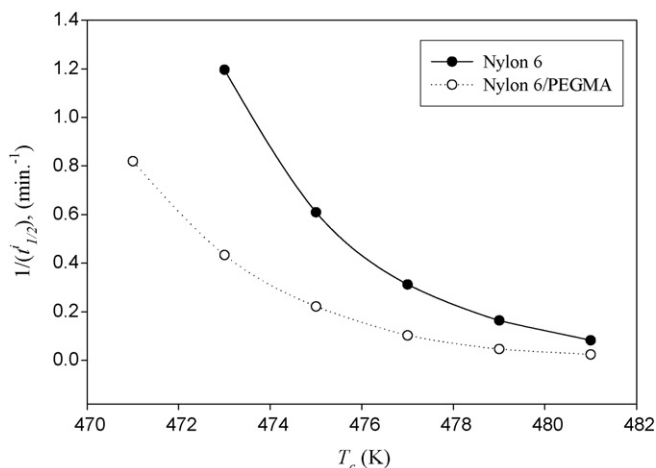


Fig. 5. $1/t_{1/2}^i$ as a function of isothermal crystallization temperature.

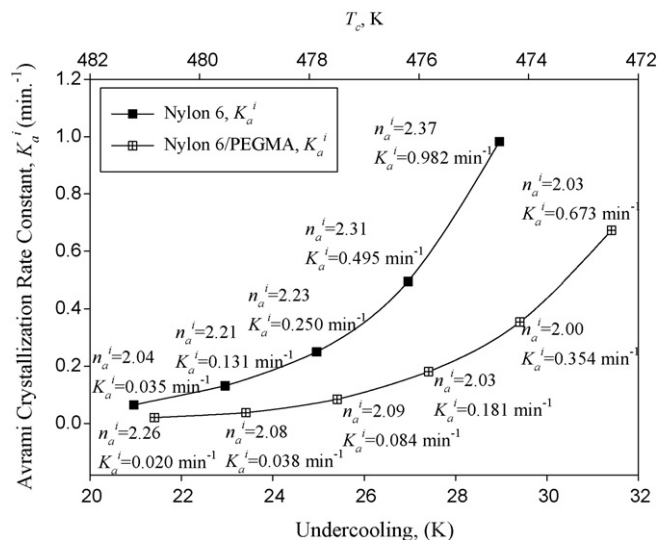


Fig. 6. Relation of undercooling and isothermal rate constants evaluated from Avrami model.

3.3.1. Avrami analysis

The Avrami equation was applied to analyze the isothermal crystallization process of polymers [17–19]:

$$X_t = 1 - \exp(-K_a t^{n_a}) \quad (3)$$

where X_t is the relative crystallinity, t is the crystallization time, K_a is the Avrami crystallization rate constant and n_a is the Avrami exponent. X_t can be calculated as the ratio between the area of the exothermic peak at time t and the total measured area of crystallization. Under isothermal crystallization, crystallization rate constant (K_a^i) and Avrami exponent (n_a^i) were found by fitting experimental data of X_t^i to Eq. (3) and the results are shown in Fig. 6. Reconstruction of Eq. (3) from the calculated K_a^i and n_a^i values (Fig. 4b) shows that Avrami model provides a good fitting.

Avrami exponent represents a parameter revealing the nucleation mechanism and growth dimension. The n_a^i values are around 2.04–2.37 for Nylon 6 and 2.03–2.23 for Nylon 6/PEGMA blend. The n_a^i values are close to the results (2.1–2.3) reported by literature [30], which is a two-dimensional growth of a spherulite. No significant changes of the values of n_a^i were found with the addition of PEGMA and thus the addition of PEGMA may not affect the geometric dimension of Nylon 6 crystal growth.

While n_a^i may be recognized as a constant with crystallization temperatures (T_c), K_a^i depends strongly on T_c . The isothermal rate constants, K_a^i , are also shown in Fig. 6 as a function of T_c for these two samples. The values K_a^i increased with decreasing T_c .

To compare crystallizability of Nylon 6 and Nylon 6/PEGMA blend, the undercooling and crystallization rate constants calculated from Avrami model are shown in Fig. 6. To reach an assigned value of rate constant, the blend needed to be imposed a higher undercooling than Nylon 6; it indicated that the crystallization rate of Nylon 6 is greater than Nylon 6/PEGMA [31]. The overall crystallization rate is governed by nucleation and dif-

fusion [32]. The reaction between Nylon 6 and PEGMA would reduce the molecular mobility and crystallization rate due to an increasing in melt viscosity.

3.3.2. Activation energy (ΔE_a^i) from isothermal crystallization

The crystallization process is assumed to be thermally activated and the crystallization rate constant K_a can be approximately described as follows:

$$\ln K_a^i = \ln K_0 - \frac{\Delta E_a^i}{RT_c} \quad (4)$$

where K_0 is the temperature-dependent pre-exponential factor, R is the gas constant and ΔE_a^i is the activation energy for the primary crystallization process which consists of the transport activation energy and the nucleation activation energy [33,34]. The ΔE_a^i are estimated from the slopes of linear plots of $\ln K_a$ against $1/T_c$ and shown in Fig. 7. The ΔE_a^i values are -76.9 and -81.0 kJ/mole for Nylon 6 and Nylon 6/PEGMA, respectively. The apparent activation energy, ΔE_a^i , cannot be further proportioned into its transport and nucleation components.

3.3.3. Nucleation parameter from isothermal thermal analysis

The overall crystallization rate should be interpreted by the combination of nucleation and growth phenomena. Hoffman–Lauritzen [13] proposed the following equation:

$$G = G_0 \exp \left[\frac{-U^*}{R(T_c - T_\infty)} - \frac{K_g}{T_c(\Delta T)f} \right] \quad (5)$$

where G is the crystallization rate parameter and G_0 is a preexponential term; $U^* = 1500$ cal/mole is the diffusional activation energy for the transport of crystallizable segments at the liquid–solid interface; R is the gas constant; $T_\infty = T_g - 30$ K and $T_g = 323$ K [33] is the hypothetical temperature below which viscous flow ceases; $\Delta T = T_m^0 - T_c$; $f = 2T_c/(T_m^0 + T_c)$ is a correction factor; K_g is the nucleation parameter which can

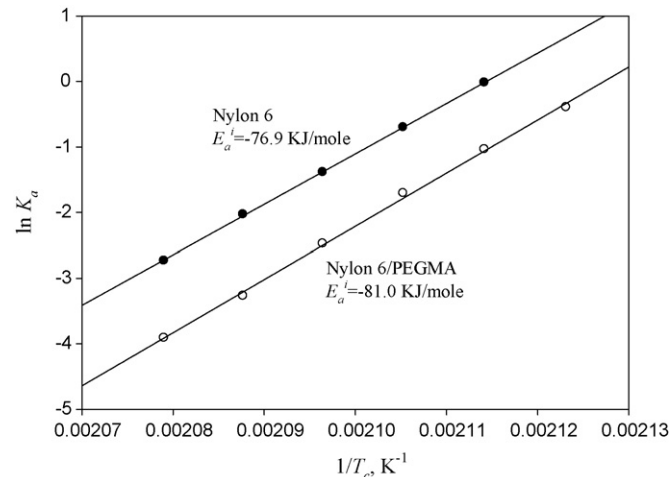


Fig. 7. Activation Energy (ΔE_a^i) from isothermal crystallization.

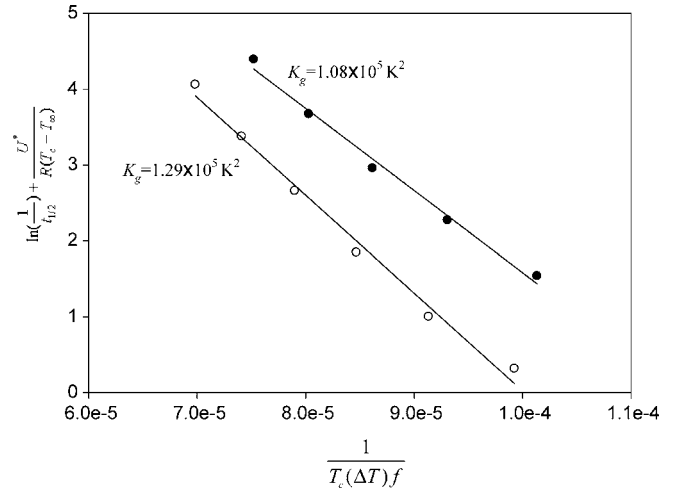


Fig. 8. Plot of $\ln(1/t^i) + (U^*/R(T_c - T_\infty))$ as a function of $\ln \psi_0 - (K_g/T_c(\Delta T)f)$.

be related to the product of lateral and folding surface free energy.

The crystallization rate parameter G is considered proportional to $t_{1/2}^i$, Eq. (5) is rewritten as:

$$\frac{1}{t^i} = G_0 \exp \left[\frac{-U^*}{R(T_c - T_\infty)} - \frac{K_g}{T_c(\Delta T)f} \right] \quad (6a)$$

or

$$\ln \left(\frac{1}{t_{1/2}^i} \right) + \frac{U^*}{R(T_c - T_\infty)} = \ln G_0 - \frac{K_g}{T_c(\Delta T)f} \quad (6b)$$

Fig. 8 demonstrates the plot of Eq. (6b) for Nylon 6 and Nylon 6/PEGMA, and the K_g values are estimated from the slope and intercept of Fig. 8. The K_g value (1.08×10^5) of neat Nylon 6 is close to the value ($0.737\text{--}1.53 \times 10^5$) reported in literatures [29,30].

The nucleation parameter (K_g) represents the free energy necessary to form a nucleus of critical size. Higher value of K_g in Nylon 6/PEGMA blend than neat Nylon 6 indicated that the motion of the Nylon 6 chains is more difficult in the blend. The result is consistent with the conclusion provided by the crystallization rate constant.

3.4. Nonisothermal crystallization kinetics

Fig. 9a shows representative DSC thermograms of nonisothermal crystallization of Nylon 6/PEGMA at different cooling rates. The exothermic peaks became wider and shifted towards lower temperature with increasing cooling rate. Table 1 lists some characteristic parameters for nonisothermal melt crystallization. For both samples, the onset of crystallization temperature (T_o), peak temperature (T_p) and end of crystallization temperature (T_∞) all shifted towards lower temperature with increasing cooling rate. The onset temperature of crystallization (T_o) and peak crystallization temperature (T_p) of Nylon 6 shift to a lower temperature, which indicates the addition of PEGMA retards the crystallization. The reciprocal half-time of

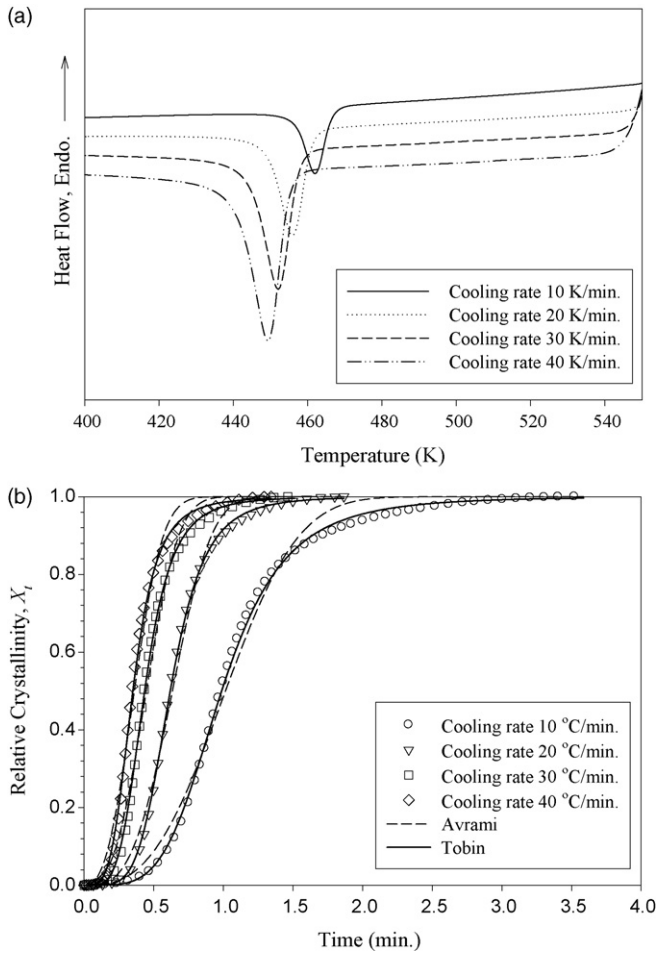


Fig. 9. DSC nonisothermal measurement. (a) Heat flow, and (b) relative crystallinity as a function of crystallization time and fitted by Avrami and Tobin models.

crystallization ($t_{1/2}^n$) is also a measure of the overall rate of nonisothermal crystallization. It also indicates the crystallization rate is reduced with the addition of PEGMA.

The relative degree of crystallinity, X_T^n , of nonisothermal crystallization was calculated as the ratio of the exothermic peak areas [35,36]:

$$X_T^n = \frac{\int_{T_0}^T [dH_c^n / dT] dT}{\int_{T_0}^{T_\infty} [dH_c^n / dT] dT} \quad (7)$$

where T is an arbitrary temperature, dH_c^n is the enthalpy of crystallization released during an infinitesimal temperature interval dT ; the relative crystallinity X_T^n is a function of temperature

Table 2
Nonisothermal Avrami and Tobin kinetics parameters

		10	3.11	0.955	0.990	0.996	4.76	1.104	0.999
Nylon 6	20	3.19	1.577	1.023	0.994	4.85	1.816	0.999	
	30	2.83	2.172	1.026	0.996	4.33	2.583	0.999	
	40	2.68	2.869	1.026	0.995	4.12	3.339	0.999	
	10	2.86	0.865	0.985	0.992	4.34	1.011	0.999	
Nylon 6/PEGMA	20	3.28	1.408	1.017	0.994	4.96	1.616	0.999	
	30	2.86	1.926	1.022	0.992	4.36	2.300	0.999	
	40	2.62	2.454	1.022	0.990	4.03	2.854	0.999	

for Nylon 6 and Nylon 6/PEGMA. During the nonisothermal crystallization process, the time, t , and temperature exhibit the following relationship:

$$t = \left| \frac{T_0 - T}{\varphi} \right| \quad (8)$$

where φ is the cooling rate. A typical relative crystallinity (X_t^n) of Nylon 6/PEGMA as a function of time is illustrated in Fig. 9b. The higher the cooling rate results in the shorter the time for completing the crystallization.

3.4.1. Avrami analysis

Avrami equation [15–17] was also employed to describe the primary stage of nonisothermal crystallization. Nonisothermal crystallization rate constant (K_a^n) and Avrami exponent (n_a^n) were found by fitting experimental data of X_t to Eq. (3) and the results are shown in Table 2.

In nonisothermal crystallization K_a^n and n_a^n do not have the same physical significance as in the isothermal crystallization because the temperature changes constantly. Assuming constant or approximately constant cooling rate, Jeziorny [37] suggested the modified Avrami to characterize the kinetics of nonisothermal crystallization:

$$\ln K_J = \frac{\ln K_a}{\varphi} \quad (9)$$

The results obtained from Jeziorny method are listed in Table 2.

Using the values thus obtained, the theoretical Eq. (4) was used and simulation results are compared to experimental data for all cooling rates examined in Fig. 9b. Deviation from the experimental data at high relative crystallinity is generally attributed to spherulite impinging effect.

Table 1
Characteristic data of nonisothermal melt crystallization exotherms for Nylon 6 and Nylon 6/PEGMA

Cooling rate φ (K/min)	Nylon 6				Nylon 6/PEGMA			
	T_0 (K)	T_p (K)	T_∞ (K)	$t_{1/2}^n$ (min)	T_0 (K)	T_p (K)	T_∞ (K)	$t_{1/2}^n$ (min)
10	473.9	466.4	447.2	0.90	471.0	461.0	435.1	0.97
20	470.6	460.6	436.9	0.54	467.2	455.9	429.9	0.61
30	467.5	457.6	426.1	0.38	463.5	452.1	418.2	0.42
40	465.2	454.1	420.2	0.29	461.2	450.3	407.5	0.34

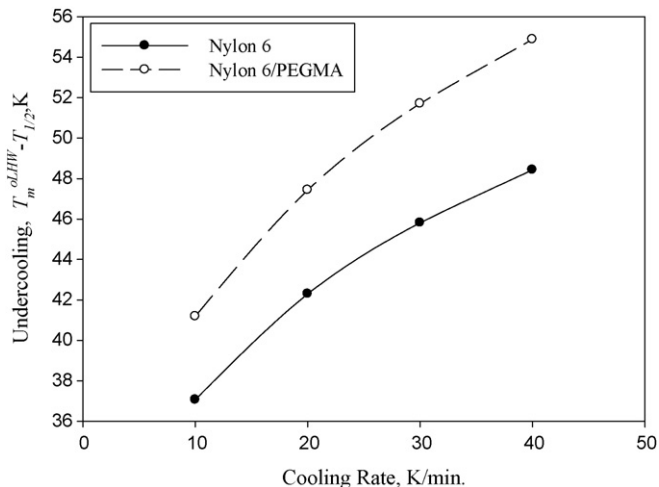


Fig. 10. Dependence of undercooling, $T_m^o - T_{1/2}$, on cooling rate.

3.4.2. Tobin analysis

Tobin [18–20] proposed the following expression to describe phase transformation kinetics with growth site impingement in order to improve the Avrami model which is suitable for the early stages of crystallization.

$$X_t = \frac{(K_t t)^{n_t}}{1 + (K_t t)^{n_t}} \quad (10)$$

where K_t is the Tobin rate constant, and n_t is the Tobin exponent. Tobin exponent n_t is not necessary an integer and is mainly governed by different types of nucleation and growth mechanism. Tobin parameters (K_t and n_t) of Eq. (10) under nonisothermal crystallization can be found by directly fitting the X_t^n data obtained from each cooling rate to equation and the results are shown in Table 2. The Tobin exponent (n_t) was found to increase with cooling rate from 4.03 to 4.96 and it was always higher than the Avrami exponent (n_a). The reconstructed relative crystallization as a function of time by adapting Tobin models, as shown in Fig. 9b, demonstrates a better fitting than Avrami model. Both Avrami and Tobin model should only be used to “describe” the nonisothermal crystallization since they are assumed to be under isothermal conditions.

Crystallizability can be compared at the same degree of undercooling. Fig. 10 shows the undercooling needed to reach 50% relative crystallization ($X_t = 0.5$), that is $T_m^o - T_{1/2}$. Higher undercooling would suggest a lower crystallizability and Fig. 10 indicated that the crystallizability of Nylon 6 is higher than the blend [32]. The results suggest that the addition of PEGMA slowed down the kinetics.

3.4.3. Effective activation energy

Several methods have been suggested to estimate the effective energy barrier in nonisothermal crystallization [38–40]. However, to ignore the negative sign in cooling process may result in errors [41]. The Friedman equation [42] is applied to nonisothermal crystallization for estimating the dependence of the effective activation energy on conversion and temperature. The

Friedman equation can be expressed as follows:

$$\ln \left(\frac{dX_t^n}{dt} \right)_{X_t^n} = \text{constant} - \frac{\Delta E_{X_t^n}}{RT_{X_t^n}} \quad (11)$$

where dX_t^n/dt is the instantaneous crystallization rate as a function of time for a given value of the relative crystallinity, R is the universal gas constant, and $\Delta E_{X_t^n}$ is the effective energy barrier of the process for a given value of X_t^n . At various cooling rates, the values of dX_t^n/dt at a specific X_t^n are correlated to the corresponding crystallization temperature at this X_t^n , that is, $T_{X_t^n}$, a straight line can be obtained by plotting dX_t^n/dt versus $1/T_{X_t^n}$ and the slope is $-\Delta E_{X_t^n}/R$.

The dependence of the effective activation energy and temperature on conversion based on Friedman equation is shown in Fig. 11. The activation energy increases with the increasing relative crystallinity in both samples, and Nylon 6/PEGMA had higher activation energy than neat Nylon 6. Nonisothermal crystallization becomes more difficult with increasing X_t^n . It also indicated that PEGMA reduced the crystallization rate.

3.4.4. Nucleation parameter from nonisothermal thermal analysis

Kishore and Vasanthakumari [21] used $G = dX_t^n/dt$ and rearranged Eq. (5) to get the following equation:

$$\frac{dX_t^n}{dt} = \frac{G_o}{\varphi} \exp \left[\frac{-U^*}{R(T - T_\infty)} \right] \exp \left[\frac{-K_g(T_m^o - T)}{2T^2(T_m^o - T)} \right] \quad (12)$$

T_p is the maximum rate which could be obtained by differentiating Eq. (12) with respect to T and equating it to zero, yielding Eq. (13):

$$K_g = \frac{U^* T_p^3 (T_m^o - T_p)^2}{R(T_p T_m^o - T_m^{o2} + T_p^2)(T_p - T_\infty)^2} \quad (13)$$

Fig. 12 shows the dependence of K_g values on T_p values resulted from different cooling rate. The K_g values increases with decreasing T_p , i.e. increases with increasing cooling rate. The values are much lower than those results obtained from isothermal crystallization and literatures [29,30]. It seems inapplicable in neat Nylon 6 and Nylon 6/PEGMA.

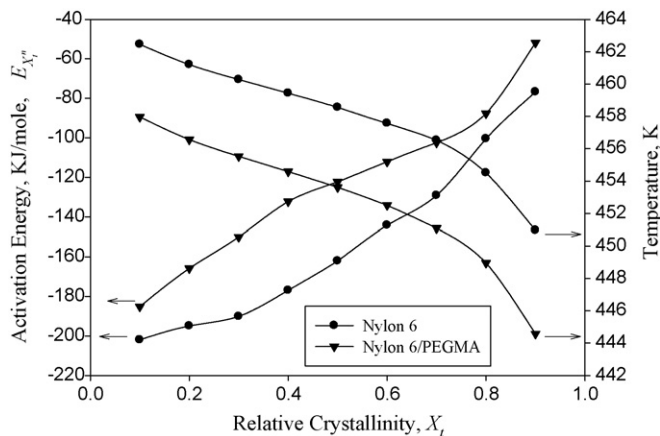


Fig. 11. Dependence of the effective energy barrier and average temperature on the extent of relative crystallinity (X_t^n).

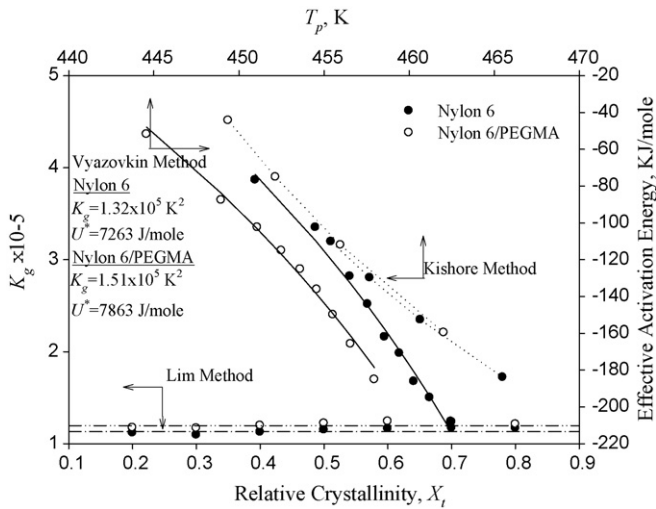


Fig. 12. K_g values calculated by Kishore, Lim, and Vyazovkin method.

Lim et al. [22] modified the Lauritzen–Hoffman equation by substituting T_c with $(T_o - \phi t)$ to measure the spherulite growth rate as a function of temperature and cooling rate in nonisothermal crystallization as following equation:

$$\ln G + \frac{U^*}{R(T_o - \phi t - T_\infty)} = \ln G_o - \frac{K_g}{(T_o - \phi t)[T_m^o - (T_o - \phi t)]f} \quad (14a)$$

$$f = \frac{2(T_o - \phi t)}{T_m^o + (T_o - \phi t)} \quad (14b)$$

G is the growth rate and G is the inversely proportional to the time to achieve a specific relative degree of crystallinity, i.e. $G \approx 1/t_{X_t^n}$ [41]. The K_g could be obtained from the slope with similar method as isothermal crystallization. Fig. 12 shows the K_g values does not show significantly change with X_t^n . The K_g values of neat Nylon 6 are $1.09\text{--}1.17 \times 10^5$ which are close to above result obtained from isothermal crystallization and literatures [29,30].

However, to assume a constant U^* for both samples does not seem reasonable because the addition of PEGMA would influence the molecular mobility. Vyazovkin et al. [23,24] used the dependence of the effective activation energy on temperature to estimate the parameters (K_g and U^*) of the Lauritzen–Hoffman theory [43] and derived the following equation:

$$\Delta E_{X_t} = -R \frac{(\ln G)}{d(1/T)} = U^* \frac{T^2}{(T - T_\infty)^2} + K_g R \frac{(T_m^o)^2 - T^2 - T_m^o T}{(T_m^o - T)^2 T} \quad (15)$$

Fig. 12 shows the dependence of the effective activation energy on temperature evaluated by replacing X_t with an average temperature, according to Vyazovkin's method [42,43]. The values K_g and U^* can be estimated by fitting Eq. (15) with the dependence of the effective activation energy on temperature, and the results are shown in Fig. 12. The K_g values obtained from

Eq. (15) are close to above results and literatures [30,31]. The higher U^* value (7863 J/mole) of Nylon 6/PEGMA than that (7263 J/mole) of neat Nylon 6 also means the addition of PEGMA retards the chain mobility and reduces the crystallization rate.

4. Conclusion

Blend of Nylon 6 and poly(ethylene-co-glycidyl methacrylate) (PEGMA) were prepared by compounding in a twin-screw extruder. The PEGMA was well dispersed in Nylon 6 from SEM morphology. Crystallization of neat Nylon 6 and Nylon 6/PEGMA was described by Avrami and Tobin models. The introduction of PEGMA slowed the kinetics of both isothermal and nonisothermal crystallization of Nylon 6 due to reduction in chain mobility because of the reaction between the epoxy groups in PEGMA and the end groups of Nylon 6 ($-\text{NH}_2$ or $-\text{COOH}$ groups). Reduction of Nylon 6 mobility also led to an increase in T_m^o . Determination of K_g and U^* values in the Hoffman–Lauritzen equation by Vyazovkin's method demonstrated that Nylon 6/PEGMA had higher K_g and U^* values indicating that the addition of PEGMA reduced the Nylon 6 mobility and decreased the crystallization rate. Vyazovkin's method is a powerful technique to study polymer crystallization and gives supportive evidence consistent with the kinetics data in the present article.

References

- [1] S.C. Manning, R.B. Moore, Polym. Eng. Sci. 39 (1999) 1921.
- [2] N.C. Liu, H.Q. Xie, W.E. Baker, Polymer 34 (1993) 4680.
- [3] A. Aróostegui, J. Nazábal, J. Polym. Sci. Polym. Phys. 41 (2003) 2236.
- [4] M. Penco, M.A. Pastorino, E. Occhiello, F. Garbassi, R. Braglia, G. Giannotta, J. Appl. Polym. Sci. 57 (1995) 329.
- [5] S.I. Lee, B.C. Chun, Polymer 39 (1998) 6441.
- [6] E.G. Koulouri, A.X. Georgaki, J.K. Kallitsis, Polymer 38 (1997) 4185.
- [7] C.H. Tsai, F.C. Chang, J. Appl. Polym. Sci. 61 (1996) 321.
- [8] Y. Pietrasanta, J.J. Robin, N. Torres, B. Boutevin, Macromol. Chem. Phys. 200 (1999) 142.
- [9] N. Torres, J.J. Robin, B. Boutevin, J. Appl. Polym. Sci. 81 (2001) 2377.
- [10] N.K. Kalfoglou, D.S. Skadas, J.K. Kallitsis, J.C. Lambert, L.V. der Stappen, Polymer 36 (1995) 4453.
- [11] S.S. Dagli, K.M. Kamdar, Polym. Eng. Sci. 34 (1994) 1709.
- [12] J.Y. Wu, W.C. Lee, W.F. Kuo, H.C. Kao, M.S. Lee, L.L. Lin, Adv. Polym. Technol. 14 (1995) 47.
- [13] J.D. Hoffman, G.T. Davis, J.I. Lauritzen Jr., in: N.B. Hannay (Ed.), Treatise on Solid State Chemistry, vol. 3, Plenum, NY, 1976, p. 497.
- [14] J.D. Hoffman, J.J. Weeks, J. Res. Nat. Bur. Stand. 66A (1962) 13.
- [15] M.J. Avrami, Chem. Phys. 7 (1939) 1103.
- [16] M.J. Avrami, Chem. Phys. 8 (1940) 212.
- [17] M.J. Avrami, Chem. Phys. 9 (1941) 17.
- [18] M.C. Tobin, J. Polym. Sci., Polym. Phys. 12 (1974) 399.
- [19] M.C. Tobin, J. Polym. Sci., Polym. Phys. 14 (1976) 2253.
- [20] M.C. Tobin, J. Polym. Sci., Polym. Phys. 15 (1977) 2269.
- [21] K. Kishore, R. Vasanthakumari, Colloid Polym. Sci. 266 (1988) 999.
- [22] B.A. Lim, K.S. McGuire, D.R. Lloyd, Polym. Eng. Sci. 33 (1993) 537.
- [23] S. Vyazovkin, N. Sbirrazzuoli, Macromol. Rapid Commun. 25 (2004) 733.
- [24] S. Vyazovkin, I. Dranca, Macromol. Chem. Phys. 207 (2006) 20.
- [25] H.H. Chang, J.S. Wu, F.C. Chang, J. Polym. Res. 1 (1994) 235.
- [26] W.B. Liu, W.F. Kuo, F.C. Chang, Eur. Polym. J. 32 (1996) 91.
- [27] E. Eder, A. Wlochowicz, J. Therm. Anal. Calorim. 35 (1989) 751.
- [28] A. Wlochowicz, M. Eder, Coll. Polym. Sci. 261 (1983) 621.
- [29] B. Burnett, W.F. McDevit, J. Appl. Phys. 28 (1957) 1001.

- [30] T.M. Wu, Y.H. Lien, S.F. Hsu, *J. Appl. Polym. Sci.* 94 (2004) 2196.
- [31] W. Weng, G. Chen, D. Wu, *Polymer* 44 (2003) 8119.
- [32] V. Causin, C. Marega, A. Marigo, L. Valentini, J.M. Kenny, *Macromolecules* 38 (2005) 409.
- [33] J.T. Xu, Y.Q. Zhao, Q. Wang, Z.Q. Fan, *Polymer* 46 (2005) 11978.
- [34] Z. Lin, Z. Huang, Y. Zhang, K. Mai, H. Zeng, *J. Appl. Polym. Sci.* 91 (2004) 2443.
- [35] M.L. DiLorenzo, C. Silvestre, *Prog. Polym. Sci.* 24 (1999) 917.
- [36] J.N. Hay, P.A. Fitzgerald, M. Wiles, *Polymer* 17 (1976) 1015.
- [37] A. Jeziorny, *Polymer* 19 (1978) 1142.
- [38] J.A. Augis, J.E. Bennett, *Therm. Anal.* 13 (1978) 283.
- [39] H.E. Kissinger, *J. Res. Nat. Bur. Stand.* 57 (1956) 217.
- [40] R.L. Takhor, *Advances in Nucleation and Crystallization of Glasses*, American Chemical Society, Columbus, 1971.
- [41] George Z. Papageorgiou, Dimitris S. Achilias, Dimitris N. Bikiaris, *Macromol. Chem. Phys.* 208 (2007) 1250–1264.
- [42] S. Vyazovkin, N. Sbirrazzuoli, *J. Phys. Chem. B* 107 (2003) 882.
- [43] H. Friedman, *J. Polym. Sci. Part C: Polym. Symp.* 6 (1964) 183.